

Flow history explains temporal and spatial variation of carbon fractionation in stream periphyton

Gabriel A. Singer, Michaela Panzenböck, Gabriele Weigelhofer, Christina Marchesani, Johann Waringer

Department of Limnology, IECB, University of Vienna, Althanstr. 14, A-1090 Vienna, Austria

Wolfgang Wanek

Department of Chemical Plant Physiology, IECB, University of Vienna, Althanstr. 14, A-1090 Vienna, Austria

*Tom J. Battin*¹

Department of Limnology, IECB, University of Vienna, Althanstr. 14, A-1090 Vienna, Austria

Abstract

We investigated factors that contribute to isotopic carbon fractionation in periphytic biofilms in a human-altered headwater stream with a flashy hydrograph. Water velocity had an important effect on periphyton $\delta^{13}\text{C}$, explaining both temporal and spatial variation. We found that water velocity averaged over a certain period before sampling, rather than the instantaneous water velocity, explained a high percentage of both temporal and spatial variation of the periphyton $\delta^{13}\text{C}$ signature. The relationship between water velocity and periphyton $\delta^{13}\text{C}$ signature was particularly influenced by individual flow events during the recent flow history. A simple model based on a flow history of 3–4 weeks reliably estimated the $\delta^{13}\text{C}$ signature of periphyton from distinct reaches. The model clearly identified signature shifts caused by the deposition of activated sludge particles from a wastewater treatment plant onto the periphytic biofilms. We highlight the high spatial and temporal variability of periphyton $\delta^{13}\text{C}$ signatures (i.e., up to 3–6‰) in a heterogeneous flow environment with inputs from a wastewater treatment plant, and we explore its implications for food web analysis.

The use of stable isotopes has greatly contributed to our understanding about the sources of organic carbon and its flow through food webs in aquatic ecosystems (Peterson and Fry 1987; Finlay 2001). However, high spatial and temporal variation associated with the $\delta^{13}\text{C}$ signature of autochthonous organic matter often limits its use to site-specific and/or date-specific approaches (Rosenfeld and Roff 1992; Zah et al. 2001) or compels one to account for observed time trends in isotopic mixing models (McCutchan and Lewis 2001, 2002). Small-scale spatial variations in autochthonous organic matter $\delta^{13}\text{C}$ signatures are not accounted for in many of these approaches and still remain poorly understood (e.g., Rosenfeld and Roff 1992; France 1995b; Zah et al. 2001). On the other hand, aquatic scientists are aware of the wide array of factors influencing carbon fractionation in primary producers (e.g., Hecky and Hesslein 1995; Finlay et al. 1999; Trudeau and Rasmussen 2003) and successfully use spatio-temporally variable autochthonous $\delta^{13}\text{C}$ signatures to identify resources of consumers and to delineate the spatial extent of aquatic food webs (Finlay et al. 2002; Melville and

Connolly 2003). Thorough understanding of spatiotemporal heterogeneity of autochthonous carbon fractionation, its underlying mechanisms, and the reliable prediction of resource $\delta^{13}\text{C}$ signatures in aquatic environments would greatly improve the application of stable carbon isotope techniques in, for example, food-web models (cf. France 1995b; Finlay et al. 2002).

The source and availability of carbon are among the primary controls of $\delta^{13}\text{C}$ signatures in aquatic primary producers (e.g., Fogel and Cifuentes 1993). Theoretically, organic carbon derived from aquatic plants has isotopic signatures close to -37‰ if full equilibrium exists between water and the atmosphere and if CO_2 (as carbon source) is available in excess. This signature should result from the two fractionation processes of the solution of gaseous CO_2 in the water and discrimination by the carbon fixation mediated by the RubisCo enzyme, with the latter being relatively greater than the former (Hecky and Hesslein 1995). However, even in fast-flowing streams, atmospheric and isotopic equilibria are rarely achieved (Raven et al. 1982; Hecky and Hesslein 1995), and the $\delta^{13}\text{C}$ signature of dissolved inorganic carbon (DIC) can vary significantly depending on the amount and source of the respired carbon (e.g., Osmond et al. 1981). Additionally, when CO_2 becomes limiting, aquatic primary producers can also actively take up HCO_3^- , a DIC species with a higher $\delta^{13}\text{C}$ signature than that of dissolved CO_2 (Mook et al. 1974).

Mass transfer through the diffusive boundary layer (and, therefore, water velocity) controls both CO_2 supply and isotopic discrimination by primary producers (Keeley and

¹ Corresponding author (tomba@pflaphy.pph.univie.ac.at).

Acknowledgments

We are grateful to the staff of the wastewater treatment plant Gresten for daily gauge readings, to S. Heintel for sample preparation, and to two anonymous reviewers for constructive comments. Financial support came from the EU-Project STREAMES (EVK1-CT-2000-00081) and a Ramon y Cajal fellowship to T.J.B. This paper is part of the fulfillment of the requirements toward an M.Sc. degree at the University of Vienna by G.A.S.

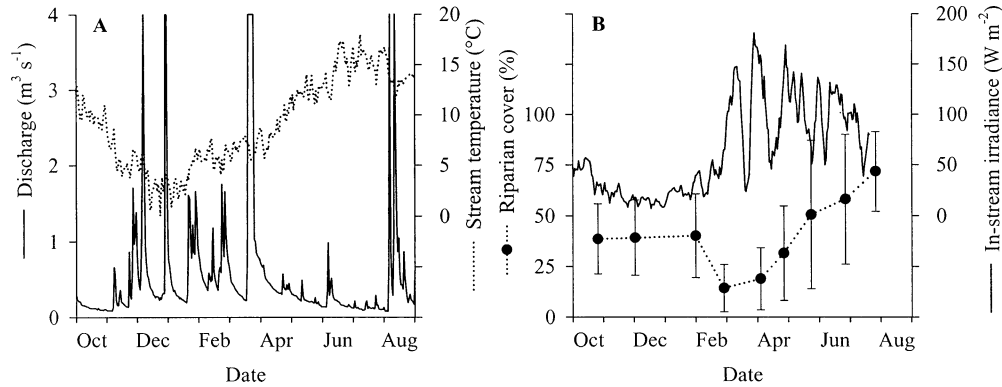


Fig. 1. (A) Discharge and streamwater temperature of the Kleine Erlauf during the study period. (B) Riparian cover as the percentage reduction of irradiance by riparian vegetation (mean \pm SD from three upstream sites) and in-stream irradiance (mean from three upstream sites).

Sandquist 1992; Hecky and Hesslein 1995; Finlay et al. 1999). Therefore, benthic algae growing under stagnant or low-turbulence conditions in lakes exhibit $\delta^{13}\text{C}$ values higher than those of phytoplankton and riverine algae growing under more turbulent or high-flow conditions (France 1995a; Hecky and Hesslein 1995). However, controversy regarding this relationship continues. For instance, no relationship between velocity and periphyton $\delta^{13}\text{C}$ signatures was found in streams with supersaturated CO_2 concentrations, low productivity, or high velocity (e.g., MacLeod and Barton 1998; Zah et al. 2001), but Trudeau and Rasmussen (2003) unequivocally demonstrated the relationship in experimental flumes with constant-flow environments. Finlay et al. (1999) argued that isotopic discrimination reflects carbon supply relative to demand and, therefore, that its relationship with water velocity can be expected to be more pronounced under higher productivity, when photosynthesis is always more carbon limited. Elucidating the relationship between periphyton $\delta^{13}\text{C}$ signatures and velocity is, however, of great importance for food-web modeling, because periphyton $\delta^{13}\text{C}$ signatures can be transmitted to herbivores (Finlay et al. 1999).

The aims of the present study were to investigate the effect of water velocity on periphyton $\delta^{13}\text{C}$ signatures in a headwater stream and to develop a model that predicts $\delta^{13}\text{C}$ signatures from flow history. Given the high temporal and spatial heterogeneity of flow, we postulated that the flow environment of periphyton during growth serves as a better predictor for $\delta^{13}\text{C}$ signature than the instantaneous water velocity. We used this model to predict temporally and spatially variable $\delta^{13}\text{C}$ signatures from spot measurements of water velocity and to discern possible effects of a wastewater treatment plant (WWTP) on the periphyton $\delta^{13}\text{C}$ signature.

Methods

We sampled periphytic biofilms from a third-order gravel stream (Kleine Erlauf, Gresten, $15^\circ 1' \text{E}$ $47^\circ 59' \text{N}$) in Austria. Catchment ($\sim 40 \text{ km}^2$) geology is characterized by calcareous limestone, and land use is strongly influenced by agriculture and forestry. Streamwater is well buffered, with pH values typically ranging from 8.0 to 8.5 and alkalinity rang-

ing from 4.4 to 4.7 mVal L^{-1} . Sampling was performed in two reaches upstream and downstream of a small-sized WWTP (2,421 equivalent inhabitants). The WWTP discharges 6 L s^{-1} into the stream, with dissolved nutrient concentrations (annual mean \pm SD) as follows: $\text{NH}_4\text{-N}$, $0.4 \pm 0.7 \text{ mg L}^{-1}$; $\text{NO}_3\text{-N}$, $13.5 \pm 7.3 \text{ mg L}^{-1}$; and $\text{PO}_4\text{-P}$, $0.8 \pm 0.9 \text{ mg L}^{-1}$. Sludge particle concentration averaged $7.4 \pm 5.3 \text{ mg L}^{-1}$, which could increase stream seston concentration by 60%.

The stream flow regime was flashy, with discharge values ranging from 75 to $4,000 \text{ L s}^{-1}$, which translates into water velocities ranging from 14 to 70 cm s^{-1} at the sampling sites (Fig. 1A). Streamwater temperature and in-stream irradiance exhibited seasonal patterns during the study period (Fig. 1). Canopy cover reduced the amount of available light by 0% to 93%, and daily mean in-stream irradiance ranged from 1.2 to 304 W m^{-2} . Benthic chlorophyll *a* (Chl *a*) ranged from 41 to 458 mg m^{-2} and from 43 to 168 mg m^{-2} in the upstream and downstream reach, respectively. Downstream nutrient concentrations were impacted by the WWTP effluent (Table 1).

Small cobbles (diameter, 5–10 cm) coated with periphyton were collected on seven occasions (October 2001 to July 2002) from the thalweg at three upstream (UP) and two downstream (DW) sites (i.e., DW1 and DW2). Upstream sites were located 500, 300, and 50 m upstream of the WWTP; downstream sites were located 100 m (DW1) and 600 m (DW6) downstream of the WWTP. We collected one upstream and triplicate downstream samples per site and date. Samples were immediately frozen and kept at -20°C . Periphyton was scraped from cobbles with a blade, dried at 50°C , and stored pending analysis.

Stream seston and sludge particles from the WWTP were sampled from study reaches and from the WWTP effluent. In the downstream reach, duplicate samples were taken at five sites that were evenly distributed from 100 to 600 m below the WWTP. Three-liter samples were filtered onto pre-combusted glass-fiber filters (Whatman GF/F) that were subsequently dried and ground.

Inorganic carbon was removed from periphyton, stream seston, and sludge particles by repeated addition of 10 N HCl. Samples were analyzed for stable carbon isotopes using

Table 1. Characteristics of the study stream. Data are given as mean \pm standard deviation.

	UP	DW 1	DW 6
Length of reach (m)	450		600
Temperature ($^{\circ}$ C)	9.27 \pm 4.25		9.37 \pm 4.29
Water velocity (cm s $^{-1}$)	41.1 \pm 18.9	45.1 \pm 18.4	47.8 \pm 19.6
In-stream irradiance (W m $^{-2}$)	61.9 \pm 52.2	96.9 \pm 84.7	67.4 \pm 61.5
Median grain size Q_{50} (mm)	29.1 \pm 8.5	25.6 \pm 7.9	31.1 \pm 6.6
AFDM* (g m $^{-2}$)	118.8 \pm 32.0	146.7 \pm 32.5	104.1 \pm 15.6
Chlorophyll a (mg m $^{-2}$)	123.8 \pm 111.1	84.5 \pm 40.4	81.3 \pm 47.1
Primary production (mg C m $^{-2}$ d $^{-1}$)	545.9 \pm 493.4	387.1 \pm 192.6	369.5 \pm 164.9
NH $_4$ -N (mg L $^{-1}$)	0.01 \pm 0.01		0.10 \pm 0.02
NO $_3$ -N (mg L $^{-1}$)	1.10 \pm 0.07		1.58 \pm 0.09
PO $_4$ -P (mg L $^{-1}$)	0.008 \pm 0.001		0.05 \pm 0.01
Conductivity (μ S cm $^{-1}$)	436 \pm 4		450 \pm 5
SPOM* load (mg L $^{-1}$)	2.6 \pm 1.3	3.1 \pm 0.9	4.2 \pm 2.0
SPOM δ^{13} C (‰)	-27.9 \pm 1.0	-27.3 \pm 1.2	-27.1 \pm 1.3
Periphyton δ^{13} C (‰)	-32.9 \pm 3.1	-29.6 \pm 5.4	-33.0 \pm 3.0

* AFDM, ash free dry mass; SPOM, suspended particulate organic matter.

continuous-flow mode in an elemental analyzer (EA 1110, CE Instruments) coupled via a ConFlo II interface (Finnigan MAT) to the gas isotope ratio mass spectrometer (Delta^{PLUS}, Finnigan MAT). High-purity CO $_2$ reference gas was calibrated to V-PDB (Pee Dee Belemnite) using the international standards IAEA-CH-6 and IAEA-CH-7 (IAEA) and was run with each analysis. The standard deviation of repeated measurements of a working standard was 0.1‰.

Chlorophyll a was extracted with acetone from aliquot samples and estimated according to the method described by Steinman and Lamberti (1996). Estimates of primary production were derived for each site and date by an empirical model using temperature and Chl a (Morin et al. 1999). Streamwater temperature was continuously recorded with submersible data-loggers (StowAway, Onset Computer Corp.) that were buried in shallow sediments, and irradiance was measured with SKYE light meters (Pyranometer Sensor SKS 1110 on SKP 2200 control unit).

Stream discharge was computed from daily gauge readings near the WWTP. Mean water velocity was derived from four to six randomly distributed measurements at the thalweg (depth, 60% below surface) with a propeller flowmeter (Ott Kleinflügel C2) at each sampling date. Sampling site-specific regressions relating mean water velocity to gauge allowed calculation of the mean water velocity for every day between sampling dates.

Benthic sediments were sampled at each site and date to derive the median grain size (Q_{50}). We then calculated site-specific critical erosion velocities for the Q_{50} (m) grain size from $v_c = 4.6 \cdot z^{1/6} \cdot Q_{50}^{1/3}$, where v_c is the critical erosion velocity (m s $^{-1}$) and z is the depth (m) (cf. Tippner 1972). Where mean water velocity was higher than erosion velocity, we assumed a flow environment mobilizing grain sizes of $<Q_{50}$ and, thus, potentially abrading periphyton.

Statistical analyses were performed with SPSS 8.0 (SPSS, Inc.) and Statistica 4.5 (Statsoft Inc.). Because data did not significantly deviate from normal distribution (Kolmogorov-Smirnov test, $p > 0.05$), we followed parametric test procedures (t -test) without previous transformation to test for differences between reaches or sites. Linear-regression co-

efficients were compared according to the method of Sokal and Rohlf (1995). For multiple comparisons between two regression lines, significance levels were adjusted according to the Dunn-Sidak method (cf. Sokal and Rohlf 1995). All data are given as mean \pm standard deviation.

Results

Periphyton δ^{13} C signatures showed distinct temporal patterns, with values ranging from -30.0‰ to -40.0‰ and from -23.2‰ to -40.4‰ in the upstream and downstream reach, respectively (Fig. 2B). Spatial within-reach variation was lower than temporal variation, with values of single sampling dates ranging within 0.3–3.9‰ and 1.0–6.4‰ in the upstream and downstream reach, respectively. Downstream samples were significantly more enriched than upstream samples (paired t -test: $t = -2.7$, degrees of freedom = 48, $p < 0.01$).

We found upstream periphyton δ^{13} C values to be related inversely to water velocity. Moreover, our data show that the amount of δ^{13} C variance that was explained increased significantly when we considered the flow history when defined as the velocity averaged over a given number of days before sampling (Fig. 3). Whereas the variation in instantaneous water velocity explained only 41% ($p < 0.01$) of the variance of periphyton δ^{13} C signature, the variation in water velocity averaged over 35 d before sampling explained 90% ($p < 0.001$) of the variance in the upstream reach (Fig. 3). Similarly, multiple linear regressions that included both the history of water velocity and its coefficient of variation (as a measure of hydrograph variability) explained between 56% ($p < 0.001$) and 92% ($p < 0.001$) of the variance of the δ^{13} C signature for flow histories encompassing 7 and 35 d, respectively (data not presented). Storm events yielding erosion velocities for Q_{50} sediments affected the trajectory describing the relationship between variance explained (r^2 of periphyton δ^{13} C vs. flow history) and duration of flow history (Fig. 3C). Including storm events in the calculation of flow history reduced the amount of variance explained when

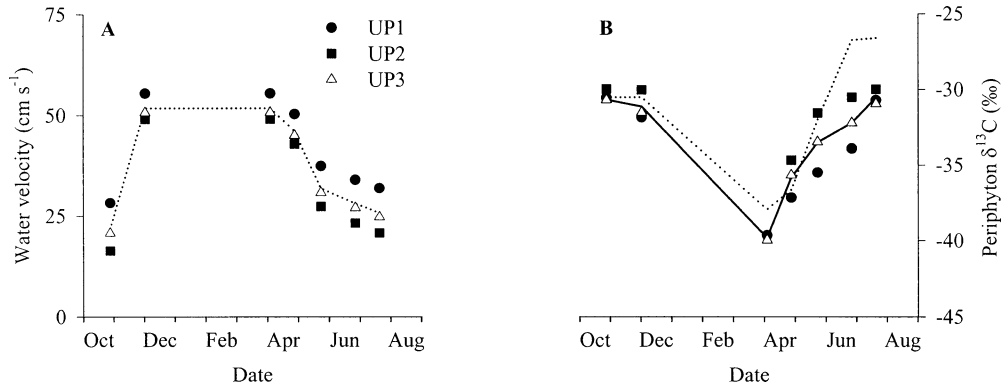


Fig. 2. (A) Water velocities in all three upstream sites (UP) during the study period. The dotted line designates average velocity. (B) Temporal and spatial variation of periphyton $\delta^{13}\text{C}$ -signature in all three upstream sites. Solid and dotted lines represent upstream and downstream average values, respectively. Symbols in (B) are the same as in (A).

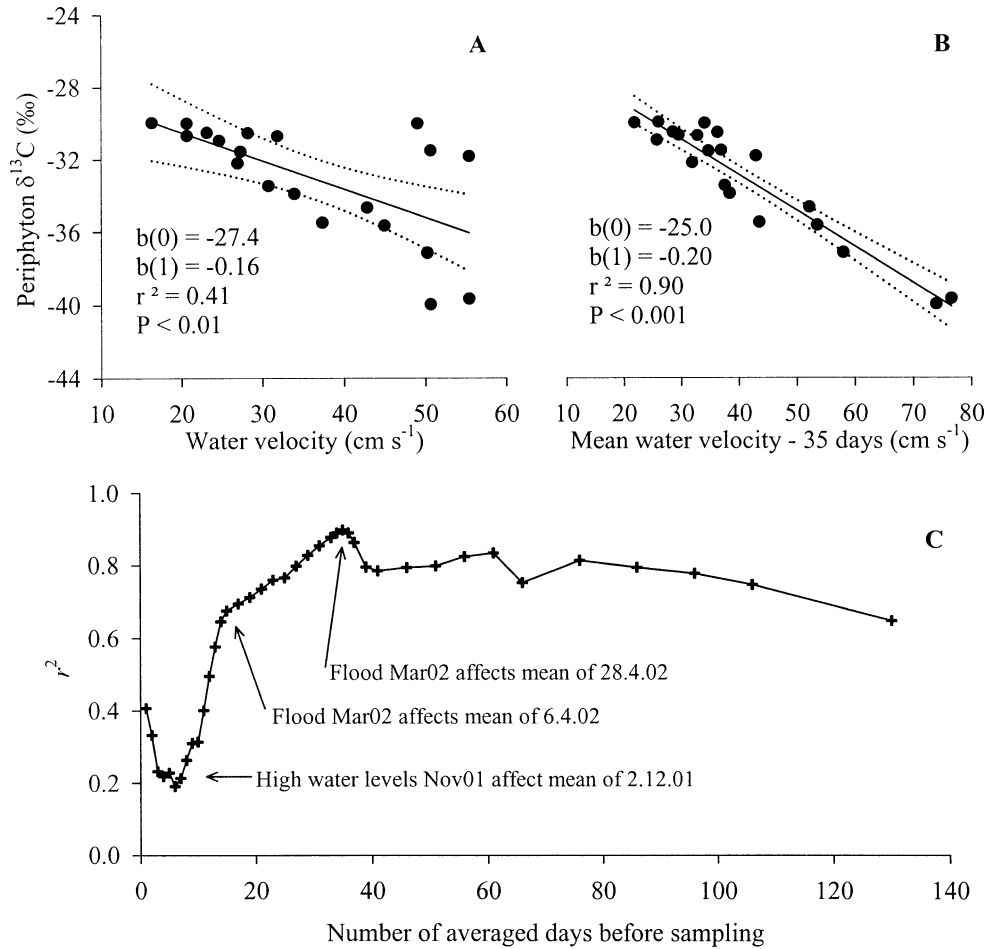


Fig. 3. Relationships between periphyton $\delta^{13}\text{C}$ -signature and (A) instantaneous water velocity and (B) flow history (35-d mean velocity) in the upstream reach. (C) Trajectory of the coefficient of determination (r^2) from the relationship between periphyton $\delta^{13}\text{C}$ -signature and flow history against duration of flow history (as the number of days before sampling).

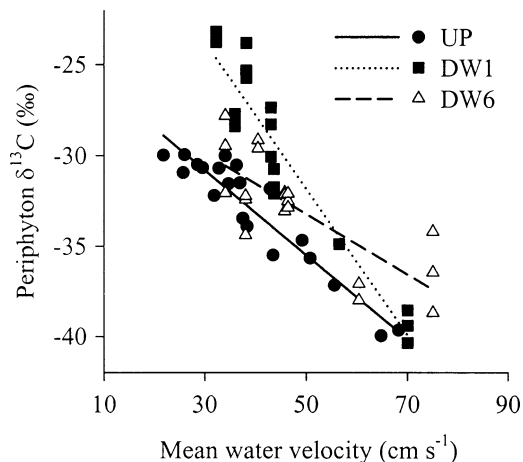


Fig. 4. Relationships between periphyton $\delta^{13}\text{C}$ and flow history. Model coefficients are given in Table 2. UP designates the upstream reach with pooled data from all three sampling sites; DW1 and DW6 designate downstream sampling sites 100 m and 600 m downstream of the WWTP, respectively.

storm-affected velocities occurred within the recent past and, thus, strongly affected mean velocity. Alternatively, the slope of the curve describing the relationship between r^2 and the number of averaged days decreased when storm events occurred in the more distant past and, thus, had less effect on the mean velocity.

Periphyton $\delta^{13}\text{C}$ signatures did not correlate with Chl *a* (Pearson's $r = 0.13$, $p = 0.62$) or with estimates of primary production (Pearson's $r = 0.23$, $p = 0.37$). Similarly, in-stream irradiance did not correlate with $\delta^{13}\text{C}$ signatures (Pearson's $r = -0.43$, $p = 0.06$) (data not presented).

We used the relationship between flow history and $\delta^{13}\text{C}$ signatures to discern possible effects of the WWTP. Flow history was expressed as the velocity averaged over the period that extends from the last storm having erosive velocities to the sampling date of periphyton, though with a maximum of 35 d. We found linear regressions relating flow history to $\delta^{13}\text{C}$ signatures yielding different slopes among the upstream reach (data from the three sites pooled) and the two downstream sampling sites (Fig. 4; Table 2). At DW1, the slope and intercept of the regression line were significantly different from those of the upstream reach and DW6.

Furthermore, we used the upstream model to predict periphyton $\delta^{13}\text{C}$ signatures at DW1 and DW6 and found significantly different residuals (observed—predicted), averaging $4.59\text{‰} \pm 2.77\text{‰}$ and $2.15\text{‰} \pm 2.07\text{‰}$, respectively (t -test, $t = 3.1$, degrees of freedom = 36, $p < 0.01$). We regarded these residuals as a “WWTP effect.” We found them (log-transformed) to correlate weakly but significantly (Pearson's $r = -0.53$, $p < 0.05$) with discharge at DW1, but no such correlation (Pearson's $r = 0.36$, $p = 0.13$) could be found at DW6.

Discussion

The present results document the temporal and spatial variation of periphyton $\delta^{13}\text{C}$ signatures in a headwater stream

Table 2. Coefficients \pm standard error for linear regression models of Fig. 4. Superscripts indicate slopes $b(1)$ differing significantly at $p < 0.01$.

	Intercept $b(0)$	Slope $b(1)$	r^2	p
UP	-23.79 ± 0.81	-0.23 ± 0.02^a	0.89	< 0.001
DW1	-11.61 ± 1.53	-0.40 ± 0.03^b	0.90	< 0.001
DW6	-24.88 ± 1.61	$-0.17 \pm 0.03^{a,b}$	0.62	< 0.001

impacted by a WWTP. Small-scale spatial variations in periphyton $\delta^{13}\text{C}$ signatures of up to 3.9‰ in the upstream reach and up to 6.4‰ in the downstream reach influenced by the WWTP are dramatic compared to a trophic shift of 0.5‰, as usually assumed in food-web studies (Peterson and Fry 1987; McCutchan et al. 2003). We found the previous water velocity record to predict this variation best, which agrees with the results of other field and experimental studies (e.g., Finlay et al. 1999; Trudeau and Rasmussen 2003).

Our results suggest that periphyton integrates shifts in carbon fractionation that occur during growth. The mechanism underlying this memory effect likely relates to the diffusional resistance of ^{13}C -DIC to both “external” and “internal” mass transfer. External mass transfer depends on the thickness of the diffusive boundary layer and, hence, on water velocity, whereas the internal mass transfer depends on the thickness and microarchitecture of periphytic biofilms (cf. Battin et al. 2003). For instance, low diffusional resistance in young and thin periphytic biofilms presumably implies good replenishment of CO_2 as a DIC source for algae, which is usually associated with $\delta^{13}\text{C}$ signatures that are depleted in ^{13}C (Raven et al. 1982). By contrast, elevated diffusional resistance in mature and thicker biofilms and, therefore, restricted replenishment of CO_2 will force algae to discriminate less between ^{12}C and ^{13}C or to shift from CO_2 to HCO_3^- as a DIC source, which are two processes that result in $\delta^{13}\text{C}$ signatures enriched in ^{13}C (Raven et al. 1982). This is the case for those algal cells that live in deeper layers of periphytic biofilms, that are exposed to CO_2 depleted in ^{12}C , and thus, that may rely predominantly on HCO_3^- . This scenario would agree with the experimental work of Trudeau and Rasmussen (2003) regarding periphyton $\delta^{13}\text{C}$ signatures. In fact, those authors found significantly different relationships between $\delta^{13}\text{C}$ signatures and velocities for periphyton grown on glass and rock substrates, and they argued that enhanced HCO_3^- availability from rocks causes this pattern. Here, it is important to note that water velocity not only influences the external mass transfer but also shapes periphytic microarchitecture (see Battin et al. 2003) and, hence, the discrimination within and among DIC sources.

Our findings of an isotopic memory in stream periphyton is, indeed, analogous to all animals whose body $\delta^{13}\text{C}$ signatures represent an integrated “nutritional history” reflecting the isotopic signatures of the food assimilated over time (Tieszen et al. 1983; Gearing 1991). Depending on the growth rate and metabolic turnover, this isotopic memory of entire animal bodies or distinct tissues will be different, with half-life estimates ranging from days to months or years (Fry and Arnold 1982; Tieszen et al. 1983). Along these lines, we acknowledge that our perception of an isotopic memory

depends on periphyton turnover rate (i.e., biomass production and losses) and variance in water velocity and, therefore, that it is most relevant in streams with highly fluctuating flow. We suspect that an isotopic memory of >30 d could result from the lower turnover of more persistent algal cells located at basal biofilm layers, which generally are less prone to physical abrasion during flood events (cf. Blenkinsopp and Lock 1994). We acknowledge that changes of DIC concentration and DIC $\delta^{13}\text{C}$ signature related to discharge fluctuations may further complicate the interpretation of our relationship between water velocity and the periphyton $\delta^{13}\text{C}$ signature.

Our results suggest that accounting for the history of velocity rather than the instantaneous velocity at sampling allows better predictions of periphyton $\delta^{13}\text{C}$ signatures. We recognize, however, that the pattern we found between flow history and periphyton $\delta^{13}\text{C}$ signature is partially shaped by the December storm with nearly erosive velocities before sampling (see Figs. 2, 3). Such nearly erosive velocities that remove the periphyton canopy without affecting its base layers could explain the observed patterns. This particular date also caused the initial decrease of the coefficient of determination (r^2) of the linear regression between water velocity and periphyton $\delta^{13}\text{C}$ signatures (Fig. 3). The exclusion of this date from regression analyses allows water velocity to explain 94% of the variance of periphyton $\delta^{13}\text{C}$ signatures within a flow history of 10 d (i.e., average of mean daily water velocity over 10 d instead of over 35 d).

Carbon fractionation in our study stream was not affected by Chl *a*, primary production, in-stream irradiance, or temperature—all factors that possibly influence photosynthesis rates (e.g., Wiencke and Fisher 1990). We suspect that these factors predominantly shape periphyton $\delta^{13}\text{C}$ signatures on larger scales. In fact, Finlay (2001) found algal $\delta^{13}\text{C}$ signatures to be positively related to watershed area and suggested that carbon limitation resulting from higher productivity along with reduced carbon availability caused ^{13}C enrichment in larger rivers. Thus, as already noted by Finlay et al. (1999), moderate photosynthesis rates along with elevated carbon demand relative to DIC supply seem to be required to discern velocity effects on $\delta^{13}\text{C}$ signatures. This could, indeed, explain why $\delta^{13}\text{C}$ signatures were not related to flow in some oligotrophic streams (cf. MacLeod and Barton 1998; Zah et al. 2001).

We attribute a substantial amount of the spatial heterogeneity of periphyton $\delta^{13}\text{C}$ signature between the two study reaches to the WWTP inputs. In fact, sludge particles ($\delta^{13}\text{C} = -25.6 \pm 0.52$) were significantly (t -test: $t = -6.6$, degrees of freedom = 7, $p < 0.001$) enriched in ^{13}C compared to the upstream seston (see Table 1). Deposition of these particles and their subsequent incorporation into biofilms (cf. Battin et al. 2003) thus would explain the $\delta^{13}\text{C}$ signature enriched in ^{13}C in the downstream periphyton. Possible effects of respiratory DIC from the WWTP effluent can be discarded, because it would deplete rather than enrich the periphyton $\delta^{13}\text{C}$ signatures (Osmond et al. 1981; Fogel and Cifuentes 1993).

We found discharge to modulate the effect of the sewage particles on periphytic $\delta^{13}\text{C}$ signatures. At low discharge, particles deposit within a short distance and, thus, produce

a high WWTP effect at DW1, whereas at high discharge, particles are transported further downstream and predominantly affect periphyton signature at DW6. Coefficients of the regression models (Fig. 4; Table 2) vary predictably according to these explanations and indicate that the deposition of sludge particles occurs, on average, within a relatively short distance (<600 m), which agrees with the average travel length of 160 m of labeled sludge particles experimentally injected into the same study reach at baseflow (70 L s⁻¹; Rauter unpubl. data). Accordingly, the observed relationship between flow history and periphyton $\delta^{13}\text{C}$ at DW1 would actually be a combination of a linear (flow history and periphyton $\delta^{13}\text{C}$) and a nonlinear (discharge and particle deposition) function. Assuming the existence of an exponential decay function (i.e., flow history vs. log-transformed periphyton $\delta^{13}\text{C}$) would increase the coefficient of determination, r^2 , from 0.89 (linear model, Table 2) to 0.94 (degrees of freedom = 17, $p < 0.001$).

Spatiotemporal variation of resource signatures can have profound implications for the study of spatially complex food webs in streams. For instance, restricted knowledge on the spatial resolution of food-web resource bases constrains both our understanding of stream ecology and our ability to understand and predict human impacts (cf. Finlay et al. 2002). Therefore, a better mechanistic understanding of spatiotemporal resource variation is required to reliably use stable isotopes in food-web studies. Our results describe the spatiotemporal variation of periphyton $\delta^{13}\text{C}$ signatures as caused by velocity changes and provide evidence toward increased spatial variation caused by nutrient point sources. This emphasizes the necessity for adequate sampling of trophic resources in heterogeneous flow environments on both a spatial and a temporal scale. For instance, $\delta^{13}\text{C}$ signatures of grazers often out-range resource signatures (G. A. Singer unpubl. data), which likely is attributable to invertebrate mobility (e.g., Finlay et al. 2002) or to poor coverage of the spatiotemporal variation of periphyton (e.g., McCutchan and Lewis 2001). Prediction of periphyton $\delta^{13}\text{C}$ signatures from past water velocity strongly suggests that flow history rather than instantaneous flow is a more robust predictor in spatiotemporally complex flow environments. Furthermore, it allows the identification of distinct patch-scale and habitat-scale flow environments with different resource signatures and facilitates carbon tracking through spatially complex food webs (cf. Finlay et al. 2002).

References

- BATTIN, T. J., L. A. KAPLAN, J. D. NEWBOLD, AND C. M. E. HANSEN. 2003. Contributions of microbial biofilms to ecosystem processes in stream mesocosms. *Nature* **426**: 439–442.
- BLENKINSOPP, S. A., AND M. A. LOCK. 1994. The impact of storm-flow on river biofilm architecture. *J. Phycol.* **30**: 807–818.
- FINLAY, J. C. 2001. Stable carbon isotope ratios of river biota: Implications for carbon flow in river food webs. *Ecology* **82**: 1052–1064.
- , S. KHANDWALA, AND M. E. POWER. 2002. Spatial scales of carbon flow in a river food web. *Ecology* **83**: 1845–1859.
- , M. E. POWER, AND G. CABANA. 1999. Effects of water velocity on algal carbon isotope ratios: Implications for river food web studies. *Limnol. Oceanogr.* **44**: 1198–1203.

- FOGEL, M. A., AND L. A. CIFUENTES. 1993. Isotopic fractionation during primary production, p. 73–98. In M. H. Engel and S. A. Macko [eds.], *Organic Geochemistry*. Plenum.
- FRANCE, R. 1995a. Carbon-13 enrichment in benthic compared to planktonic algae: Food-web implications. *Mar. Ecol. Prog. Ser.* **124**: 307–312.
- . 1995b. Critical examination of stable isotope analysis as a means for tracing carbon pathways in stream ecosystems. *Can. J. Fish. Aquat. Sci.* **52**: 651–656.
- FRY, B., AND C. ARNOLD. 1982. Rapid $^{13}\text{C}/^{12}\text{C}$ turnover during growth of brown shrimp (*Penaeus aztecus*). *Oecologia* **54**: 200–204.
- GEARING, J. N. 1991. The study of diet and trophic relationships through natural abundance ^{13}C , p. 201–217. In D. C. Coleman and B. Fry [ed.], *Carbon isotope techniques*. Academic.
- HECKY, R. E., AND R. H. HESSLEIN. 1995. Contribution of benthic algae to lake food webs as revealed by stable isotope analysis. *J. N. Am. Benthol. Soc.* **14**: 631–653.
- KEELEY, J. E., AND D. R. SANDQUIST. 1992. Carbon: Freshwater plants. *Plant Cell Environ.* **15**: 1021–1035.
- MACLEOD, N. A., AND D. R. BARTON. 1998. Effects of light intensity, water velocity, and species composition on carbon and nitrogen stable isotope ratios in periphyton. *Can. J. Fish. Aquat. Sci.* **55**: 1919–1925.
- MCCUTCHAN, J. H., JR., AND W. M. LEWIS, JR. 2001. Seasonal variation in stable isotope ratios of stream algae. *Verh. Int. Ver. Theor. Angew. Limnol.* **27**: 3304–3307.
- , AND ———. 2002. Relative importance of carbon sources for macroinvertebrates in a Rocky Mountain stream. *Limnol. Oceanogr.* **47**: 742–752.
- , C. KENDALL, AND C. C. MCGRATH. 2003. Variation in trophic shift for stable isotope ratios of carbon, nitrogen, and sulfur. *Oikos* **102**: 378–390.
- MELVILLE, A. J., AND R. M. CONNOLLY. 2003. Spatial analysis of stable isotope data to determine primary sources of nutrition for fish. *Oecologia* **136**: 499–507.
- MOOK, W. G., J. C. BOMMERSON, AND W. H. STAVERMAN. 1974. Carbon isotope fractionation between dissolved bicarbonate and gaseous carbon dioxide. *Earth Planet. Sci. Lett.* **22**: 169–176.
- MORIN, A., W. LAMOUREUX, AND J. BUSNARDA. 1999. Empirical models predicting primary productivity from chlorophyll a and water temperature for stream periphyton and lake and ocean phytoplankton. *J. N. Am. Benthol. Soc.* **18**: 299–307.
- OSMOND, C. B., N. VALAANE, S. M. HASLAM, P. UOTILA, AND Z. ROKSANDIC. 1981. Comparisons of $\delta^{13}\text{C}$ values in leaves of aquatic macrophytes from different habitats in Britain and Finland: Some implications for photosynthetic processes in aquatic plants. *Oecologia* **50**: 117–124.
- PETERSON, B. J., AND B. FRY. 1987. Stable isotopes in ecosystem studies. *Annu. Rev. Ecol. Syst.* **18**: 293–320.
- RAVEN, J., J. BEARDALL, AND H. GRIFFITHS. 1982. Inorganic C-sources for *Lemanea*, *Cladophora*, and *Ranunculus* in a fast-flowing stream: Measurements of gas exchange and of carbon isotope ratio and their ecological implications. *Oecologia* **53**: 68–78.
- ROSENFELD, J. S., AND J. C. ROFF. 1992. Estimation of the carbon base in southern Ontario streams using stable isotopes. *J. N. Am. Benthol. Soc.* **11**: 1–10.
- SOKAL, R. R., AND F. J. ROHLF. 1995. *Biometry. The principles and practice of statistics in biological research*. Freeman.
- STEINMAN, A., AND G. LAMBERTI. 1996. Biomass and pigments of benthic algae, p. 295–313. In R. L. G. Hauer [ed.], *Stream ecology: Field and laboratory exercises*. Academic.
- TIESZEN, L. L., T. W. BOUTTON, K. G. TESDAHL, AND N. A. SLADE. 1983. Fractionation and turnover of stable carbon isotopes in animal tissues: Implications of $\delta^{13}\text{C}$ analysis of diet. *Oecologia* **57**: 32–37.
- TIPPNER, M. 1972. Beitrag zur Ermittlung von Gesetzmäßigkeiten der Geschiebebewegung im Oberrhein zwischen Freistatt und Worms. *Deutsche Gewässerkundl. Mitt.* **16**: 18–105.
- TRUDEAU, V., AND J. B. RASMUSSEN. 2003. The effect of water velocity on stable carbon and nitrogen isotope signatures of periphyton. *Limnol. Oceanogr.* **48**: 2194–2199.
- WIENCKE, C., AND G. FISHER. 1990. Growth and stable carbon isotope composition of cold-water macroalgae in relation to light and temperature. *Mar. Ecol. Prog. Ser.* **65**: 283–292.
- ZAH, R., P. BURGHERR, S. M. BERNASCONI, AND U. UEHLINGER. 2001. Stable isotope analysis of macroinvertebrates and their food sources in a glacier stream. *Freshwat. Biol.* **46**: 871–882.

Received: 20 January 2004
 Accepted: 7 October 2004
 Amended: 1 November 2004